AIP | Applied Physics Letters

Local structure of Cu x Zn2− x TiO4 inverse spinel

J. Ruiz-Fuertes, T. Bernert, M. He, B. Winkler, V. L. Vinograd, and V. Milman

Citation: Applied Physics Letters **105**, 071911 (2014); doi: 10.1063/1.4893458
View online: http://dx.doi.org/10.1063/1.4893458
View Table of Contents: http://scitation.aip.org/content/aip/journal/apl/105/7?ver=pdfcov
Published by the AIP Publishing

Local structure of $Cu_xZn_{2-x}TiO_4$ inverse spinel

J. Ruiz-Fuertes,[1,a)] T. Bernert,[1] M. He,[1] B. Winkler,[1] V. L. Vinograd,[2] and V. Milman[3]
[1]*Geowissenschaften, Goethe-Universität, Altenhöferallee 1, 60438 Frankfurt am Main, Germany*
[2]*Forschungszentrum Jülich GmbH, 52425 Jülich, Germany*
[3]*Dassault Systèmes BIOVIA, 334 Science Park, Cambridge CB4 0WN, United Kingdom*

(Received 21 July 2014; accepted 7 August 2014; published online 20 August 2014)

Structural and vibrational changes due to the incorporation of Cu in the $Cu_xZn_{2-x}TiO_4$ inverse spinel solid solution have been investigated by X-ray diffraction, Raman spectroscopy, and *ab initio* calculations. Both X-ray diffraction and Raman spectroscopy show that the structure remains cubic while the unit-cell volume decreases on Cu^{2+} incorporation. The compositional dependencies of the Raman frequencies and linewidths indicate the incorporation of Cu^{2+} into tetrahedral sites. The A_{1g} tetrahedral mode frequency becomes independent on composition for $x > 0.6$. This is attributed to the limited incorporation of Cu^{2+} in the tetrahedral sites at Cu-rich compositions. *Ab initio* calculations with quasi-random structures reveal only a slight energetic preference of Cu^{2+} for octahedral over tetrahedral sites. © *2014 AIP Publishing LLC*.
[http://dx.doi.org/10.1063/1.4893458]

Zinc titanates, pure or doped with transition metals, have been extensively investigated as transparent conductive oxides,[1] sensors,[2] microwave dielectrics,[3,4] and as solid state fuel cells.[5,6] The cubic ($Fd\bar{3}m$) polymorph with an inverse spinel structure is the most stable of four phases of Zn_2TiO_4.[7–10] Due to its structure, Zn_2TiO_4 is a versatile host material, ideal for engineering optical and magnetic properties.[11] In the inverse spinel structure, half of the Zn^{2+} cations occupy the 8*a* tetrahedral sites, and the other half share the 16*d* octahedral sites with 8 Ti atoms. Doping with spin-unpaired 3*d* transition metals results both in a bandgap decrease due to the admixture of metal 3*d* and O 2*p* orbitals at the top of the valence band[12] and the appearance of magnetism.[13,14] An excellent element to incorporate into the $A_xZn_{2-x}TiO_4$ solid solution is Cu^{2+}, which has one electron less than Zn^{2+}. Crystal-field theory[15] suggests that Cu is −63.7 kJ/mol more stable in the octahedral than in the tetrahedral coordination and therefore is expected to fully reside in the octahedral sites, substituting for Zn. Incorporating Cu^{2+} leads to a Jahn-Teller (JT) distortion of the coordination polyhedra, which further breaks the degeneracy of the partially occupied e_g (t_{2g}) energy levels. This distortion, linked to the magnetism and superconductivity in some compounds,[16,17] can lead to a symmetry reduction to a tetragonal structure after the alignment of all the JT distorted axes of the polyhedra below the JT transition temperature T_{JT}. However, the X-ray diffraction (XRD) study of Robbins and Darcy[18] has shown that $CuZnTiO_4$ remains cubic down to 80 K. Nestour *et al.*[13] have employed relative XRD intensities to investigate the local structure and the incorporation of Cu^{2+} in $Zn_{1-x}Cu_xAl_2O_4$ normal spinel. However, this method is not well suited for studying the incorporation of Cu^{2+} in the $Cu_xZn_{2-x}TiO_4$ inverse spinel as Cu^{2+} substitutes Zn instead of Ti and the electronic configuration of Cu^{2+} and Zn^{2+} differs by only one electron, resulting in very similar XRD structure factors.

In this Letter, we study the local structure of the $Cu_xZn_{2-x}TiO_4$ solid solution with Raman spectroscopy, powder XRD and *ab initio* calculations.

$Cu_xZn_{2-x}TiO_4$ ($x = 0$, 0.2, 0.4, 0,5, 0.6, 0.7, 0.8 and 0.9) was synthesized by a solid state reaction from 2N pure ZnO, CuO, and TiO_2 powders. After 24 h of ball milling,[19] the starting materials were compacted and then sintered at 800 °C for 24 h. XRD diffractograms were measured using a PANalytical X'Pert PRO diffractometer with Cu $K\alpha_1$ wavelength monochromatized with a Ge (111) crystal. Rietveld refinements were carried out with GSAS[20,21] and gsaslanguage.[22] Raman spectra were acquired in quasi-backscattering configuration with a Renishaw spectrometer (1800 grooves/mm) using a Nd:YAG laser ($\lambda = 532$ nm) focused with a 20× objective and a notch filter that let us measure above 120 cm^{-1} from the laser line. Samples changed color from white to dark brown upon Cu incorporation. In order to avoid sample overheating, we used a laser power of 20 mW up to $x = 0.6$ and of 2 mW for $x = 0.7$, 0.8, and 0.9. Calculations were performed with the density functional theory (DFT) plane wave pseudopotential package CASTEP.[23] Spin polarized geometry optimization calculations were performed with the Wu-Cohen density functional[24] and the on-the-fly-generated ultrasoft pseudopotentials from Accelrys Materials Studio 7, using a kinetic energy cut-off of 700 eV. Reciprocal space was sampled according to the Monkhorst-Pack scheme[25] with the maximal distance of 0.03 $Å^{-1}$ between *k*-points.

XRD patterns at ambient conditions of $Cu_xZn_{2-x}TiO_4$ for $x = 0.2$ and 0.9 are shown in Fig. 1(a) together with Rietveld refinements.[26] Apart from a few weak Bragg reflections from a silicate contamination below 1 wt. % produced during ball milling, and some CuO also below 1 wt. %, all reflections correspond to the cubic spinel phase for all Cu contents up to $x = 0.9$. We therefore believe that the compositions of the products are close to the nominal values. We unsuccessfully tried the synthesis for $x = 1$. We conclude that the solid solution is not stable at $x > 0.9$. The lattice parameter $a = 8.452$ Å, previously reported for $CuZnTiO_4$,[27] suggests a content of $x = 0.6$ instead of $x = 1$ if compared to our

a)Electronic address: ruiz-fuertes@kristall.uni-frankfurt.de

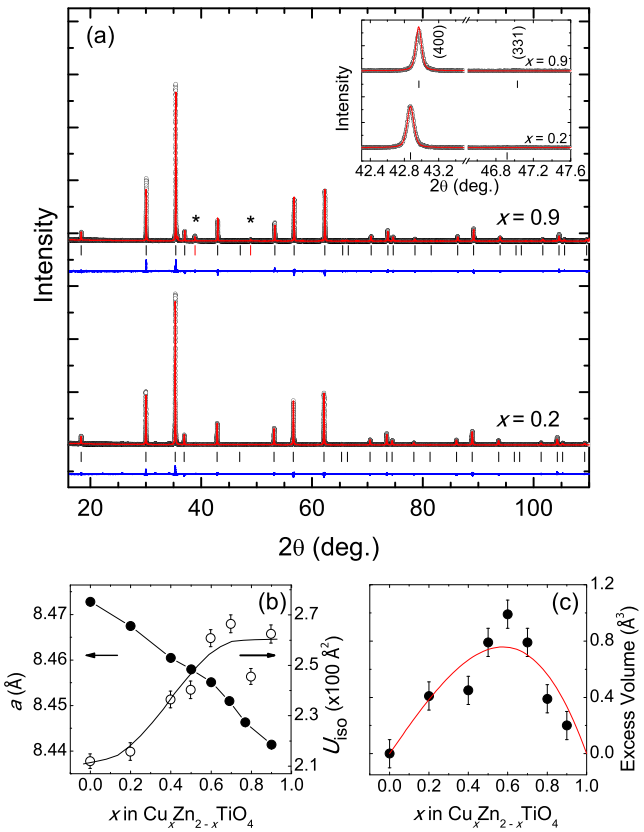

FIG. 1. (a) X-ray diffractograms of $Cu_xZn_{2-x}TiO_4$ with Rietveld refinements for $x = 0.2$, and 0.9. Asterisks show the reflections of CuO. The inset shows the (400) and (331) reflections. (b) Lattice parameter a as a function of Cu concentration and O thermal displacement parameter U_{iso}. Black lines are guides to the eye. (c) Unit-cell volume excess with respect to ideal mixing. The continuous line represents a two-parameter Margules fit.

results. Unfortunately, Tare *et al.*[27] do not show any diffractogram that might help to determine the origin of this discrepancy. On increasing Cu content, the only change observed is the shift of the Bragg reflections toward higher 2θ angles (Fig. 1(a)). This is due to a decrease of a, as shown in Fig. 1(b), where the thermal displacement parameter U_{iso} of the O atoms is also shown. The decrease of a has been previously observed in other spinel Zn-Cu solid solutions, like $Zn_{1-x}Cu_xAl_2O_4$,[13] and it is attributed to the polarizing effect of Cu^{2+} due of the JT effect. The variation of a with composition deviates from Vegard's law behavior, showing an excess volume.[28,29] The excess volume is shown in Fig. 1(c) and is asymmetric with a maximum at $x = 0.6$ that can be modeled with a subregular two-parameter Margules model[30] with $\omega_1 = 3.3(5)$ and $\omega_2 = 1.7(3)$ Å^3 per unit cell. Recalculated to one exchangeable cation, these values correspond to $\omega_1 = 0.027(3)$ and $\omega_2 = 0.013(2)$ J bar^{-1}mol^{-1}. These excess parameters appear to be comparable in the magnitude to the excess volume parameters measured, for example, in the pyrope-grossular garnets $Mg_xCa_{3-x}Al_2Si_3O_{12}$.[31] However, the excess volumes in the Ca, Mg, Fe, Mn-garnets correlates with the misfit in the ionic radii of the exchangeable atoms,[32] and is especially large for Mg-Ca solid solutions. In contrast, the ionic radii of four- and six-fold coordinated Zn^{2+} and Cu^{2+} are nearly identical.[33] Thus, the relatively large excess volume measured in this spinel solid solution cannot be attributed to a size mismatch effect. The compositional dependence of the U_{iso} (Fig. 1(b)) is indicative of an increase in the static disorder of the O atoms on increasing Cu-incorporation. At $x > 0.6$, the static disorder, which is due to the JT distortion of the coordination polyhedra on Cu-incorporation, ceases to increase. This is exactly the behavior we deduce from the Raman spectra (see below). We suggest that the observed excess volume is correlated with a distortion of the spinel structure due to the JT effect in CuO_4 and CuO_6 polyhedra, which increases non-linearly with the concentration of Cu. This result will be further supported later by Raman spectroscopy results. It is worth to point out the absence of the (331) reflection in $Cu_xZn_{2-x}TiO_4$ diffraction patterns. The intensity ratio between the (400) and the (331) reflections is very sensitive to the spinel inversion, with the (331) usually showing an intensity similar to the (400) in most normal spinels like $ZnAl_2O_4$.[13] For Zn_2TiO_4, an analysis of the structure factors shows that the intensity ratio I_{331}/I_{400} would be of around 10% if it was a normal spinel, and around 0.1% for complete inversion. Therefore, the absence of the (331) reflection in $Cu_xZn_{2-x}TiO_4$ shows that the structure remains in a completely inverse spinel structure with the Ti^{4+} cations occupying only the octahedral positions. Considering the long-range nature of XRD and the disorder of the distorted polyhedra occupied by Cu^{2+}, only a local probe, such as Raman spectroscopy, might yield additional information about the structural effect of incorporating Cu^{2+} in $Cu_xZn_{2-x}TiO_4$.

Raman spectra of $Cu_xZn_{2-x}TiO_4$ are shown in Fig. 2 with the mode assignment of Wang *et al.*[34] for Zn_2TiO_4. The cubic spinel structure has five $A_{1g} + E_g + 3F_{2g}$ Raman active modes and four F_{1u} modes which are infrared active. Due to the complete inversion of Zn_2TiO_4, the disorder locally breaks the translational symmetry, resulting in band broadening and the appearance of additional bands.[35] In fact, in

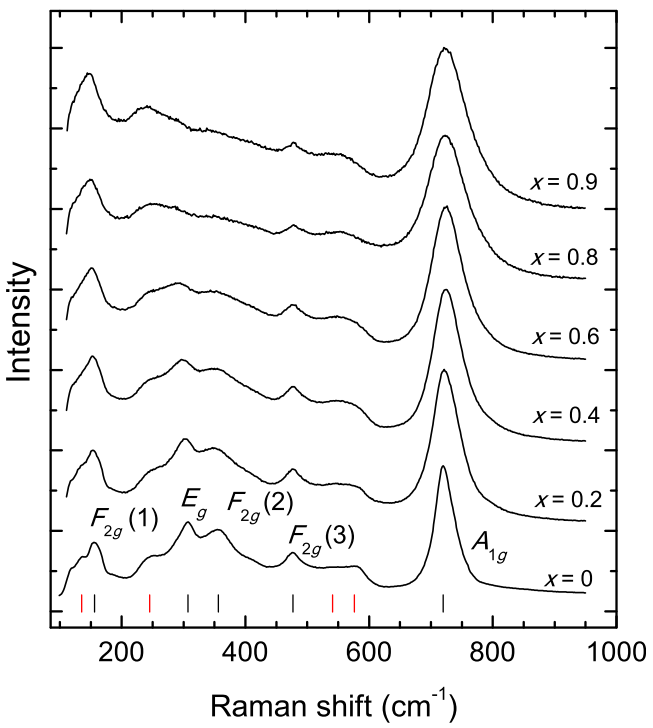

FIG. 2. Raman spectra of $Cu_xZn_{2-x}TiO_4$ with their Raman modes assignment (black tick marks).[34] Four extra bands (red ticks) may be F_{1u} modes.

Fig. 2, one can see four additional modes for $x=0$, which might be the four F_{1u} modes. However, the absence of infrared studies of Zn_2TiO_4 prevents any further mode assignments. Normalized to the intensity of the most intense A_{1g} mode, in Fig. 2, we see that the increase of the Cu-content results in peak broadening and a frequency shift. Up to $x=0.6$, the low-frequency modes shift to lower frequencies, the $F_{2g}(3)$ remains unaffected, and the A_{1g} shifts to higher frequencies. For higher Cu concentrations, the main difference consists in the change of the dependence of the E_g and A_{1g} modes on further Cu incorporation that we will discuss later. The F_{2g} modes in $CuCr_2Se_4$ involve motions of both cations and anions,[36] with the $F_{2g}(1)$ mode being sensitive to the mass of the divalent cation. In our case, with Cu and Zn having similar masses, the frequency and the width of this mode would not provide much information about the local effect of Cu incorporation. The E_g and A_{1g} modes involve only motions of the O atoms, with the A_{1g} mode being a breathing mode of the AO_4 tetrahedra and the E_g double degenerate mode being due to tangential displacement of the O with respect to the A-O bonds. In the spinel structure, the tetrahedra share only corners and thus should behave as relatively rigid units. Therefore, their vibrational modes are expected to be insensitive to Cu incorporation if Cu^{2+} occupies the octahedral sites only.[15] However, as we do observe significant changes in the Raman spectra, our observations challenge this assumption.

Profile fittings of the E_g, $F_{2g}(2)$, and A_{1g} modes for $x=0$ and 0.6, together with a schematic drawing of the mode eigenvectors are shown in Fig. 3, while the full width at half maximum (FWHM, Γ) and peak positions as determined from the fits are given in Fig. 4. Fig. 3 shows the intensity drop of the Raman bands with increasing Cu content. This cannot be observed in Fig. 2, which for clarity shows normalized spectra. A description of the E_g mode, due to its low intensity and proximity to the $F_{2g}(2)$ mode, is strongly dependent on the background removal. A reasonable fit required two Gaussians up to $x=0.6$. Above $x=0.6$, the frequency of this mode could be estimated but not Γ. The A_{1g}

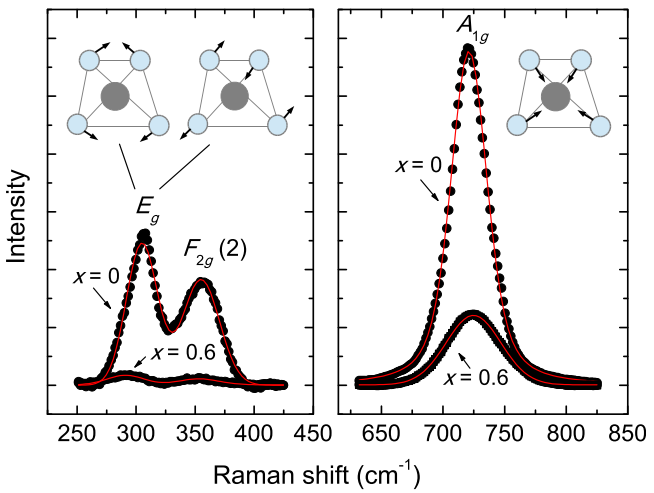

FIG. 3. Line-profile fits (continuous lines) for the E_g and A_{1g} Raman modes at $x=0$, and 0.6. The corresponding eigenvectors for the A_{1g} and the E_g modes are shown. The O atoms are represented in blue, and Zn atoms are in grey.

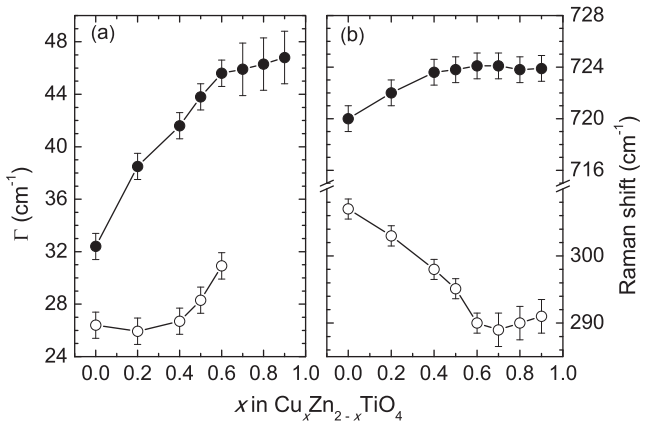

FIG. 4. (a) Full width at half maximum, Γ and (b) Raman shifts for the E_g (open circles) and A_{1g} (solid circles) tetrahedral modes of $Cu_xZn_{2-x}TiO_4$. Black lines are guides to the eye.

mode, as expected in oxide spinels, does not overlap with any other mode, and therefore, a reliable analysis of its lineshape is possible. There are several mechanisms that can give rise to lineshape broadening of a Raman mode. Gaussian line broadening is mainly due to either the instrumental resolution, which is intrinsic and therefore affects all Raman modes ($2\,cm^{-1}$ in our case), or due to a disorder[35] present in spinels. Lorentzian line broadening is mostly produced by finite phonon lifetimes either due to anharmonicity or due to lattice imperfections commonly present in solid solutions.[37] For the A_{1g} mode profile fit, a Pseudo-Voigt function was used. We found that starting with a Gaussian component of $\sim$50% for $x=0$, the lineshape gradually broadens and becomes more Gaussian up to $x=0.6$, where it can be fit with only one Gaussian function (Fig. 3). With 50% Lorentzian character for $x=0$, the A_{1g} mode appears to have anharmonic decay channels probably due to some lattice defects. However, the Gaussian broadening of the A_{1g} mode shown in Fig. 4(a) indicates that the incorporation of Cu^{2+} produces a disorder increase in the tetrahedral sites rather than an increase of lattice defects. This is consistent with the observation that the FWHM of the Bragg reflections are composition-independent (Fig. 1(a)). Due to the tetrahedral origin of this mode, this disorder must take place also in the tetrahedral site. This suggests that some Cu^{2+} is incorporated in tetrahedral sites resulting in the broadening of the A_{1g} mode, due to the contribution of two modes with very similar frequencies.[38] From $x=0.7$, Γ keeps increasing (Fig. 4), but more slowly. The incorporation of Cu^{2+} in tetrahedral sites in spinels has been previously observed,[13,14] although those studies were performed on normal spinels with no available octahedral sites for Cu^{2+}. In the present case of the inverse spinel $Cu_xZn_{2-x}TiO_4$, the partitioning of Cu into both tetrahedral and octahedral sites seems to be in contradiction to the estimated octahedral preference of -63.7 kJ/mol.[15] This site preference has been estimated as the difference of the crystal-field stabilization energy in the octahedral and tetrahedral sites determined by $d \rightarrow d^*$ optical absorption spectroscopy in different compounds.[15]

Here, the site preference is investigated with the help of *ab initio* calculations. The energy difference between an inverse and a normal spinel cannot be straightforwardly

computed from first principles as in the inverse spinel Zn and Ti are disordered over the octahedral sites. In calculations with periodic boundary conditions, this disorder needs to be approximated. The use of the "virtual crystal approximation" will not allow a correct local distortion of the Cu-containing polyhedra.[39,40] Hence, the disordered cation distribution is modeled with the help of quasi-random (QR) structures.[41] The search for QR structures has been performed by random swaps of octahedral Zn and Ti within a $1\times1\times1$ supercell with the composition of $(Zn,Ti)ZnO_4$. The criterium for the quasi-randomness was that the frequencies of *AA*, *AB*, *BA*, and *BB* pairs ($A=$Zn and $B=$Ti) at all cation-cation distances within the supercell were as close as possible to their theoretical probabilities in a completely random solid solution. Practically, the deviation was counted for *AB*-type pairs only. The structures were scored according to the following equation:

$$S=\frac{1}{2}\sum_{n=1}^{3}Z_n\left(f_{AB,n}^{exp}-f_{AB,n}^{teo}\right)^2, \quad (1)$$

where $f_{AB,n}^{exp}$ and $f_{AB,n}^{teo}$ are the current and the theoretical frequencies, respectively, and Z_n is the coordination number at the *n*-th distance. In the spinel structures, the cation to cation coordination numbers are 6, 12, and 12 for the first, second, and third neighbors of octahedral sites, respectively. In a $1\times1\times1$ supercell of the Zn_2TiO_4 inverse spinel only three pairs with different distances can be distinguished. Three structures with the lowest scores were selected from ~10 000 tested configurations. These QR structures will give the best possible representation of the structural and energetic properties of a perfectly disordered phase for the size of our supercell. The computed diffraction pattern intensities of the (331) Bragg reflection of the QR structure with the inverse configurations were 2% of the intensity of the (400) reflection. This confirms that our approach is reasonable.

The total energy of the inverse spinel has then been calculated as the average of the energies of the three best QR structures. The energy preference of the inverse spinel over the normal configuration is −0.2 eV per formula unit. Hence, the DFT-model confirms the experimental observation that the inverse structure is the ground state structure. The site preference energy of Cu^{2+} was computed as the difference in the total energies of QR structures in which a single Cu defect per unit cell was placed either in the octahedral or tetrahedral sites. We found that Cu^{2+} in an octahedral site is energetically more stable than the structure with Cu^{2+} in a tetrahedral site. However, contrary to crystal-field estimations,[15] we found that the energy difference between both structures with different Cu^{2+} sites is only −0.06 eV per Cu atom (~−6 kJ/mol). The small site preference energy supports our interpretation of the Raman spectroscopy data, which favors the partitioning of a certain unknown fraction of Cu into the tetrahedral site. We find that the effect of introducing one Cu^{2+} in a tetrahedral or an octahedral site per unit cell results both in their JT distortion and an average ~0.02% bond distance decrease. This can be correlated with the blueshift observed for the A_{1g} mode up to $x=0.6$. From our calculations, we obtain that the distortion of an octahedron on Cu-incorporation does not affect much the surrounding tetrahedra. The redshift of the tetrahedral E_g mode and the octahedral, $F_{2g}(1)$ and $F_{2g}(2)$ modes is related to the distortion of the polyhedra. Therefore, the redshift of the E_g mode up to $x=0.6$ can be explained by the entropy driven migration of some (unknown) fraction of Cu^{2+} in the tetrahedral sites. The $F_{2g}(3)$ mode, due to *A*-O tangential displacements, is unaffected by Cu incorporation. As mentioned before, for $x>0.6$, the behavior of some modes changes. In particular, the E_g mode blueshifts and the frequency of the A_{1g} mode becomes composition-independent with its Γ increasing more slowly with the increase of Cu (Fig. 4). Given the tetrahedral character of the E_g and A_{1g} modes and the effect that Cu^{2+} has on the tetrahedral sites, the change in the behavior of these two modes leads us to conclude that at a total Cu-concentration of $x=0.6$, the maximal amount of Cu^{2+} is already incorporated in the tetrahedral sites. The incorporation of Cu only in the octahedral sites above this composition would result in the decrease of the lattice parameter at a constant tetrahedral bond decrease. This results in a redshift rate decrease of the A_{1g} frequency as *a* decreases, a small change of Γ as the result of a constant tetrahedral disorder, and a blueshift of the E_g frequency. Further, the difficulty on incorporating Cu in the tetrahedral sites above $x=0.6$ would have an effect on the relative distortion of the structure, which would continue increasing due to the increase in the total Cu. Above $x=0.6$, this relative distortion is expected to proceed at a lower rate as it would depend on the JT distortion of the octahedral sites only. The maximum of the relative distortion is thus expected to occur at $x=0.6$. We argue that the dependence of the excess volume on composition shown in Fig. 1(c) correlates with this effect.

In conclusion, we have performed a Raman spectroscopy study of the $Cu_xZn_{2-x}TiO_4$ solid solution that has been complemented with XRD and *ab initio* calculations. The analysis of the Raman active modes reveals that some Cu^{2+} is incorporated in tetrahedral sites, at least up to $x=0.6$. This is consistent with the calculated small energetic preference for octahedral over tetrahedral coordination for Cu^{2+}. Accurate site-occupancies might be obtained from neutron diffraction experiments and such experiments are currently planned.

J.R.-F. thanks the Alexander von Humboldt Foundation for a postdoctoral fellowship and O. Gomis for the critical reading of the manuscript.

[1]S. Takai, Y. Asahi, and T. Esaka, J. Electrochem. Soc. **147**, 272 (2000).
[2]B. L. Zhu, C. S. Xie, W. Y. Wang, K. J. Huang, and J. H. Hu, Mater. Lett. **58**, 624 (2004).
[3]B. Li, Z. Yue, L. Li, J. Zhou, and Z. Gui, J. Mater. Sci.: Mater. Electron. **13**, 415 (2002).
[4]S. Butee, A. R. Kulkarnia, O. Prakasha, R. P. R. C. Aiyarb, K. Sudheendrand, and K. C. R. Jamesdi, Mater. Sci. Eng. B **168**, 151 (2010).
[5]T. Esaka, T. Ikebe, and M. Kamata, Solid State Ionics **76**, 237 (1995).
[6]I. Parezanovic, E. Strauch, and M. Spiegel, J. Power Sources **135**, 52 (2004).
[7]F. H. Dulin and D. E. Rase, J. Am. Ceram. Soc. **43**, 125 (1960).
[8]O. Yamaguchi, M. Morimi, H. Kawabata, and K. Shimizu, J. Am. Ceram. Soc. **70**, C97 (1987).
[9]U. Steinike and B. Wallis, Cryst. Res. Technol. **32**, 187 (1997).
[10]Y. Inaguna, A. Aimi, Y. Shirako, D. Sakurai, D. Mori, H. Kojizani, M. Akaogi, and M. Nakayama, J. Am. Chem. Soc. **136**, 2748 (2014).

[11]S. Butee, A. R. Kulkarnia, O. Prakasha, R. P. R. C. Aiyarb, I. Wattamwar, D. Bais, K. Sudheendrand, and K. C. J. Raju, Mater. Sci. Engineer. B **176**, 567 (2011).
[12]J. Ruiz-Fuertes, D. Errandonea, F. J. Manjón, D. Martínez-García, A. Segura, V. V. Ursaki, and I. M. Tiginyanu, J. Appl. Phys. **103**, 063710 (2008).
[13]A. L. Nestour, M. Gaudon, G. Villeneuve, R. Andrissen, and A. Demourgues, Inorg. Chem. **46**, 2645 (2007).
[14]D. Shoemaker and R. Seshadri, Phys. Rev. B **82**, 214107 (2010).
[15]R. G. Burns, *Mineralogical Applications of Crystal Field Theory* (Cambridge University Press, Cambridge, 1993), Vol. 5.
[16]J. G. Bednorz and K. A. Müller, Z. Phys. B: Condens. Matter **64**, 189 (1986).
[17]E. Pavarini, I. Dasgupta, T. Saha-Dasgupta, O. Jepsen, and O. K. Andersen, Phys. Rev. Lett. **87**, 047003 (2001).
[18]M. Robbins and L. Darcy, J. Phys. Chem. Solids **27**, 741 (1966).
[19]Ball milling was performed at 300 r.p.m. in an agate milling vessel of a volume of 80 ml using agate balls (balls to powder mass ratio of 10:1) in a planetary ball mill (Fritsch, pulverisette 7, premiumline).
[20]A. Larson and R. V. Dreele, Los Alamos National Laboratory Report LAUR, 2006, p. 86.
[21]B. H. Toby, J. Appl. Crystallogr. **34**, 210 (2001).
[22]S. C. Vogel, J. Appl. Crystallogr. **44**, 873 (2011).
[23]S. J. Clark, M. D. Segall, C. J. Pickard, P. J. Hasnip, M. J. Probert, K. Refson, and M. C. Paynei, Z. Kristallogr. **220**, 567 (2005).
[24]Z. Wu and R. E. Cohen, Phys. Rev. B **73**, 235116 (2006).
[25]H. J. Monkhorst and J. D. Pack, Phys. Rev. B **13**, 5188 (1976).
[26]From the Rietveld refinements, we obtain that the fractional coordinate of the O atom, *u*, almost does not change from 0.259 under Cu incorporation.
[27]M. P. Tare, R. R. Tripathi, S. Sampath, and S. M. Tare, Bull. Mater. Sci. **13**, 191 (1990).
[28]L. Vegard, Z. Phys. **5**, 17 (1921).
[29]A. R. Denton and N. W. Ashcroft, Phys. Rev. A **43**, 3161 (1991).
[30]N. A. Gokcen, J. Phase Equilib. **17**, 50 (1996).
[31]A. Bosenick and C. Geiger, J. Geophys. Res.: Solid Earth **102**, 22649 (1997).
[32]C. A. Geiger, Am. Mineral. **85**, 893 (2000).
[33]R. D. Shannon, Acta Crystallogr. A **32**, 751 (1976).
[34]D. Z. Wang, S. K. Saxena, and C. S. Zhai, Phys. Rev. B **66**, 024103 (2002).
[35]V. V. Ursaki, F. J. Manjon, I. M. Tiginyanu, and V. E. Tezlevan, J. Phys.: Condens. Matter **14**, 6801 (2002).
[36]V. G. Ivanov, M. N. Iliev, Y.-H. A. Wang, and A. Gupta, Phys. Rev. B **81**, 224302 (2010).
[37]Y.-I. Kim, S. Cadars, R. Shayib, T. Proffen, C. S. Feigerle, B. F. Chmelka, and R. Seshadr, Phys. Rev. B **78**, 195205 (2008).
[38]M. Guc, V. V. Ursaki, I. V. Bodnar, D. V. Lozhkin, E. Arushanov, V. Izquierdo-Roca, and A. Pérez-Rodríguez, Mater. Chem. Phys. **136**, 883 (2012).
[39]B. Winkler, V. Milman, and C. J. Pickard, Mines Mag. **68**, 819 (2004).
[40]D. J. Wilson, B. Winkler, E. A. Juarez-Arellano, A. Friedrich, K. Knorr, C. J. Pickard, and V. Milman, J. Phys. Chem. Solids **69**, 1861 (2008).
[41]A. Zunger, S.-H. Wei, L. G. Ferreira, and J. E. Bernard, Phys. Rev. Lett. **65**, 353 (1990).